

P. EGIZABAL*, A. GARCÍA ROMERO**, A. TORREGARAY***

ANALYSIS OF THE SOLIDIFICATION AND PROPERTIES OF PLASTER CAST AL BASED COMPOSITES

ANALIZA KRZEPNIĘCIA I WŁAŚCIWOŚCI ODLEWANYCH KOMPOZYTÓW NA BAZIE ALUMINIUM

The present work deals with aspects related to the solidification and properties of an Al-Si10Mg/SiC_{20p} alloy cast in plaster moulds. Several strategies were followed to shorten its solidification time such as embedding copper tubes into the mould to make circulate cooling fluids immediately after the casting step. The analysis of cooling curves provided valuable information on the effect of the particles on solidification events. The precipitation of different phases of the MMC takes place at higher temperatures and earlier than in the case of the non reinforced alloy. Particles affect the solidification pattern of the alloy and play a noticeable role in the precipitation of the phases. This fact should be taken into account to design the filling and feeding systems correctly and for modelling and processing parameters as well as in thermal treatments. Eventually samples were obtained under the highest solidification rate conditions to analyse the microstructure and tensile properties of the MMC material.

Keywords: F3S.20S, MMCs, lost wax, plaster casting, solidification

Praca przedstawia aspekty związane z krzepnięciem i właściwościami stopów Al-Si10Mg/SiC_{20p} odlewanych w formach gipsowych. Aby skrócić czas krzepnięcia stopu testowano kilka strategii, takich jak osadzanie rur miedzianych w formie aby umożliwić obieg cieczy chłodzących natychmiast po odlaniu stopu. Analiza krzywych chłodzenia dostarczyła cennej informacji na temat wpływu cząstek na proces krzepnięcia. Wydzielanie różnych faz w kompozytach metalowo-ceramicznych odbywa się w wyższych temperaturach i wcześniej, niż w przypadku nieumacnianego stopu. Cząstki wpływają na schemat krzepnięcia stopu i odgrywają zauważalną rolę w wydzieleniu faz. Fakt ten powinien być brany pod uwagę przy projektowaniu prawidłowego systemu zalewania formy, modelowaniu parametrów procesu, jak również obróbki cieplnej. Na koniec pobrano próbki otrzymane przy najwyższej szybkości krzepnięcia do analizy mikrostruktury i właściwości wytrzymałościowych kompozytu metalowo-ceramicznego.

1. Introduction

Particulate reinforced MMCs are combinations of a metal or alloy and particles of a second phase deliberately introduced to improve its properties. The most notable large size and volume commercial use so far is in braking systems of trains and cars, but they have also been successfully used as other components in automotive and aerospace industries as well as the electronic industry in applications such as components for helicopters, golf club shafts and heads, horseshoes, bicycle frames, car pistons, tyre studs etc. [1]

The present article deals with the study of MMCs produced through a variant of the lost wax process known as rubber plaster moulding (RPM). Lost wax foundry processes produce high added value castings

with intricate geometries and good surface quality and they are very suitable for the production of complex aeronautical and electronic components [2-4]. The heat dissipation capacity of plaster is low and this aspect must be taken into account as the solidification rate controls the grain size and the particle distribution and clustering tendency of MMCs.

Several authors have studied the solidification of MMCs [5-13] and it is demonstrated that the presence of the particulates may lead to some of the following phenomena: i) Some particulates may act as heterogeneous solidification nuclei of different phases depending on the chemical nature of the constituents of the alloy and process conditions. ii) Depending on solidification aspects particulates may be either engulfed or pushed

* FUNDACIÓN INASMET, PASEO MIKELETEGI 2, 20009 DONOSTIA

** UPV/EHU, ESCUELA UNIV. DE INGENIERÍA TÉCNICA MINERA, 48902 BARACALDO

*** UPV/EHU, DPTO.ING. MINERA, MET. Y CIENCIA DE MATERIALES, 48012 BILBAO

by the growing dendrites, iii) Reduction of latent heat during solidification. Reduction of undercooling and solidification times, iv) Ceramic particles tend to produce a shortening of the associated cooling curve and an increase in the eutectic growth temperature of Al-Si alloys as well as a decrease in the measured latent heat during solidification. Furthermore the particles play a role in the mass and thermal transfers and they may also act as nucleation sites.

2. Experimental details

Materials Al-Si10Mg/SiC_{20p}

A commercial MMC produced by the company Durcalcan called F3S.20S, based on the Al-Si10Mg alloy and with 20 vol. % of SiC particles, has been used to carry out the work. The unreinforced Al-Si9Mg alloy was also cast and studied as a reference for comparison purposes. No silicon modifiers or grain refiners were used.

The composition of both materials is presented in the Table 1.

TABLE 1

Composition of the two alloys studied

Material /wt.%	Si	Fe	Cu	Mn	Mg	Zn	Ti	SiC (vol.%)
F3S.20S	9.4	0.12	0.01	0.01	0.57	0.01	0.09	20
Al-Si9Mg	9.5	0.15	0.05	0.12	0.42	0.05	0.15	-

Analysis of the solidification

Two different strategies were tested to decrease the solidification rate of the composite material: Application of a liquid nitrogen jet on the external surface of the mould immediately after the casting step and the circulation of cool water through copper tubes embedded in the plaster mould. The solidification curves were recorded through a time-temperature recording system based on the use of plaster cups that incorporate a small type-K thermocouple with a precision of $\pm 2,2^{\circ}\text{C}$ protected by a glass tube. Figure 1 shows the commercial sand cup this system is based on. The first step was to produce the plaster cups and to adapt the thermocouples to them. The cups were produced by casting the plaster/water mixture into silicone moulds that had been obtained using the commercial sand cups as models. The glass covered thermocouples of the commercial sand cups were extracted and located in the plaster cups to record the T during the solidification stage. A commercial software NOVACAST ATAS allows the data acquisition and produces the corresponding T-t curves. Figure 2 shows the final assembly to record the solidification curves. All the final castings were produced in the same conditions:

Mould material:	MCP15 plaster from R&R (UK)
Plaster/water ratio:	80/100
Mould temperature:	200°C
Casting temperature:	730°C

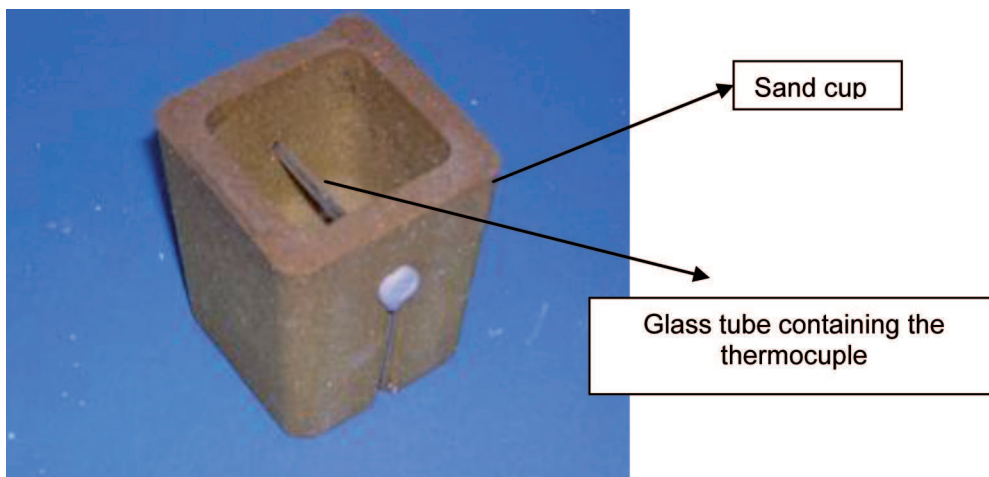


Fig. 1. Commercial sand cup with detail of thermocouple's location



Fig. 2. Plaster cups mounted on the data acquisition device, the aluminium alloy has already been cast into the cup on the left

Figure 3 shows a general view of the plaster mould cooled by circulating cold water tested. A copper tube was located in each of the half-moulds at a distance of 5-10 mm from the surface of the mould. The mould was filled in 7 seconds and the water flow was activated 38 seconds later. In the case of the test using liquid nitrogen the filling time was 12 seconds and the nitrogen was directed to the surface of the mould after 38 seconds.

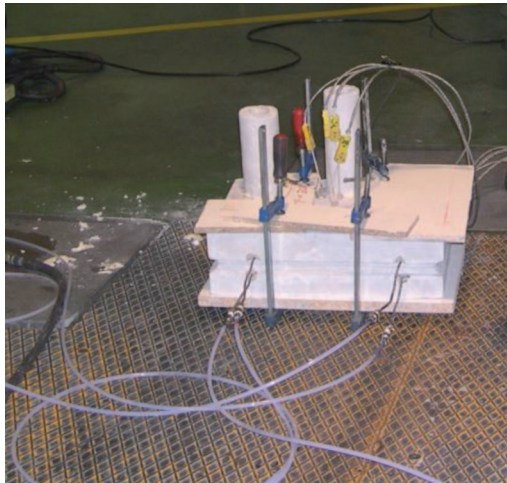


Fig. 3. Detail of the thermocouples and the water tubes connected to the copper ones embedded in the two half-moulds

The final casting was a heat dissipating part with a weight of and the following dimensions $236,5 \times 77,5 \times 10$ mm and a weight of 500 grams.

Finally the last trial was made by the simultaneous use of nitrogen and a vacuum pump. To facilitate the application of vacuum some holes were made in the outer face of the lower half-moulds.

Measurement of grain size

To measure the grain size specimens were submitted to chemical etching and the measurements were made following the procedures established by the Centre Technique des Industries de la Fonderie (CTIF) in France [14]. The alloys were attacked with an iron chloride FeCl_3 . The images obtained with an optical microscope were compared to a series of standard macrographies ($\times 10$) to determine their grain size range (SG). The latter parameter can be directly converted into grain size ranges following the equivalences shown by the mentioned procedure.

3. Results and discussion

Figure 4 shows the solidification curves obtained with the $\text{Al-Si10Mg/SiC}_{20p}$ alloy in different cooling conditions.

The curves provide information about solidification events and solidification rates. Average cooling rates were calculated through the slope of the curves in the straight line associated with the primary phase solidification. Table 2 shows the cooling rates obtained with the different methods. It can be seen that the strategy of embedding copper tubes through which a water flow is applied after the casting step provides the largest cooling rate.

TABLE 2

Cooling rates of $\text{Al-Si10Mg/SiC}_{20p}$ alloy in plaster moulds

- | | |
|----|---|
| 1) | Cooling rate without any cooling system $0,5-0,8^\circ\text{C/s}$ |
| 2) | Cooling rate by using water cooled copper tubes $2,2^\circ\text{C/s}$. |
| 3) | Cooling rate with liquid N_2 $1,6^\circ\text{C/s}$. |

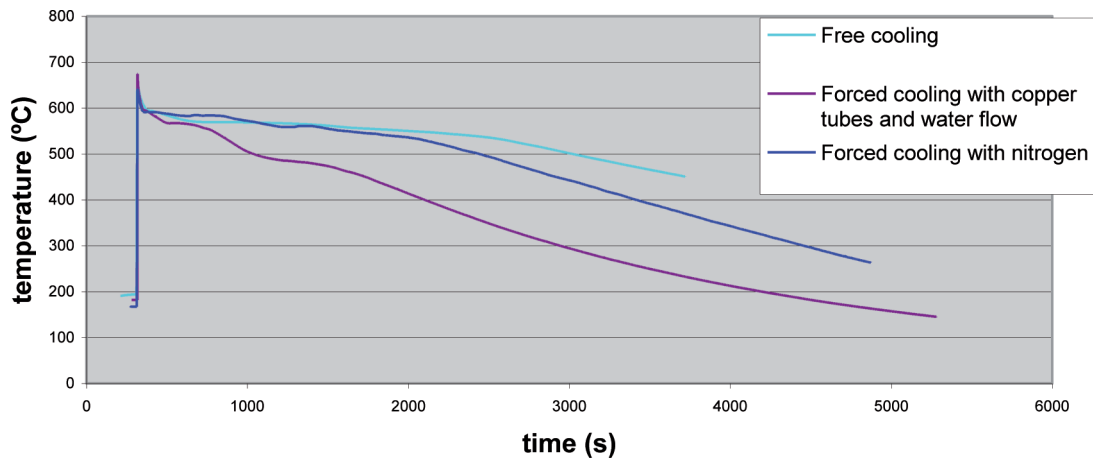


Fig. 4. Solidification curve T-t of the reinforced Al-Si10-Mg/SiC_{20P} alloy with different cooling strategies

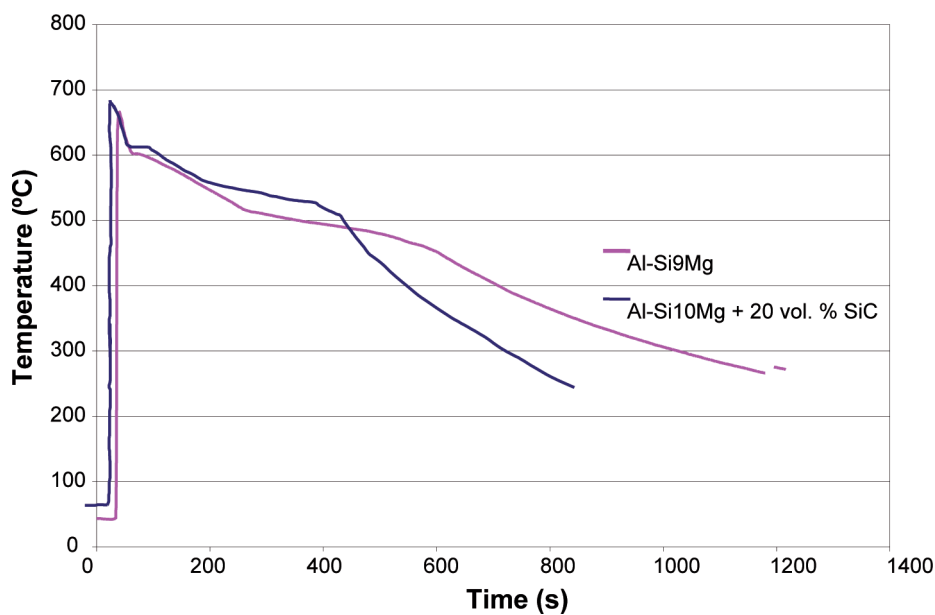


Fig. 5. Solidification curves of plaster cast Al-Si9Mg and Al-Si10Mg/SiC_{20P} alloys

Figure 5 shows the cooling curve of the alloys without any artificial cooling.

The comparison of the curves may be used to identify the differences in the precipitation of the main phases during solidification. Changes in the slopes of the curves are associated with the release of latent heat related to exothermic phase changes that can be correlated with the precipitation of intermetallic phases, initiation of the solidification of the melt and development of dendritic networks. The comparison of the curves of the composite alloy and the corresponding unreinforced alloy provides interesting information that may be useful to control their behaviour during thermal treatment and their final microstructure. The comparison of the curves in Fig. 5 shows that the solidification of the composite material is faster as the cooling curves are shorter than those of the unreinforced alloy. Nevertheless the first major

solidification event, the formation of the dendritic α -Al network starts earlier in the unreinforced alloy. It takes place around 606°C in the Al-Si9Mg alloy and at 595°C in the MMC case. This difference has been previously studied by other authors that explain it by the decrease in the nucleation potential of the primary phase due to the presence of SiC particles and the high interfacial energy associated with the Al/SiC interface and the lower thermal dissipation capacity of the composite material [5,8,11]. At the same time the amount of released latent heat measured as the area under the curves is clearly lower. This event has been studied by other authors that obtained similar results [5] and is related with the presence of 20 vol.% of SiC particles that do not present any phase change transformations during solidification. The presence of the particles also affects the rest of solidification events such as the eutectic solidification and precip-

itation of Fe based intermetallics. The curves show four main slope changes that may be associated with main solidification events of hypoeutectic Al-Si alloys following the studies carried out by different authors [5-6, 9-10, 15-16]. The curves reflect that the presence of SiC particles may play a role in the nucleation of Al-Fe-Si intermetallics such as Al_5FeSi and $Al_{15}(Fe,Mn)_3Si$ that begin at around $595^\circ C$ in comparison with $589^\circ C$ in the case of the Al-Si9Mg alloy. Similarly the onset of the eutectic reaction takes place at around $565^\circ C$ in the case of the composite material and at $542^\circ C$ in the case of the unreinforced alloy and eventually the precipitation of the Mg_2Si phase takes place at around $520^\circ C$ in the case of the Al-Si10Mg + 20 vol.% alloy, $40^\circ C$ higher than in the case of the unreinforced alloy. These results are in agreement with the solidification studies of metal matrix composites carried out by other authors and are mainly related to the nucleation potency variations and the lower latent heat associated with the presence of the SiC particles. These data must be taken into account when defining the design of the mould feeding systems for this kind of composites as well as to optimise the subsequent thermal treatments. Eventually it is clearly appreciated that the curve of the composite material is clearly shorter than that of the unreinforced alloy.

Microstructure analysis

Figures 6 and 7 show the microstructure of the Al-Si10Mg and the reinforced Al-Si10Mg/SiC_{20p} cast without any rapid cooling system applied and at the same casting conditions. The grain size of the α -aluminium dendrite is smaller (in the range of $315-500\ \mu m$) than that of the unreinforced alloy, around $500-800\ \mu m$. This result agrees with the results of Nagarajan et al. [17] that cast SiC reinforced Al-Si alloys in plaster moulds even though there seems to be a large disagreement among different studies that claim both increases [5] and decreases in the grain size [4]. Figure 7 shows that most of the SiC particles have been pushed by the solidification front and are mainly located in the grain boundary region together with Fe based intermetallics. The silicon eutectic phase appears unmodified in the Fig. 6 and slightly modified in Fig. 7. On the other hand the presence of SiC particles seems to have a positive effect on the distribution of microporosity. Figure 8 shows the presence of some large pores in the structure of the Al-Si9Mg alloy while not such pores have been apprehended in the composite material. Al-Fe-Si intermetallics typical of this alloy can be seen as dark grey needle-shaped phases distributed across the sample.

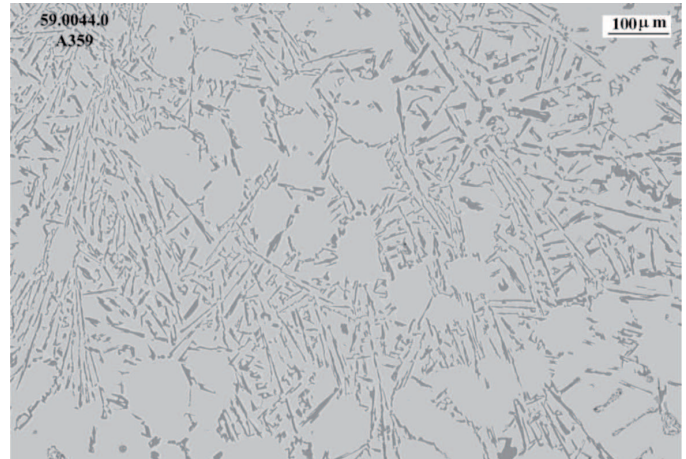


Fig. 6. Microstructure of the Al-Si9Mg alloy cast in plaster mould

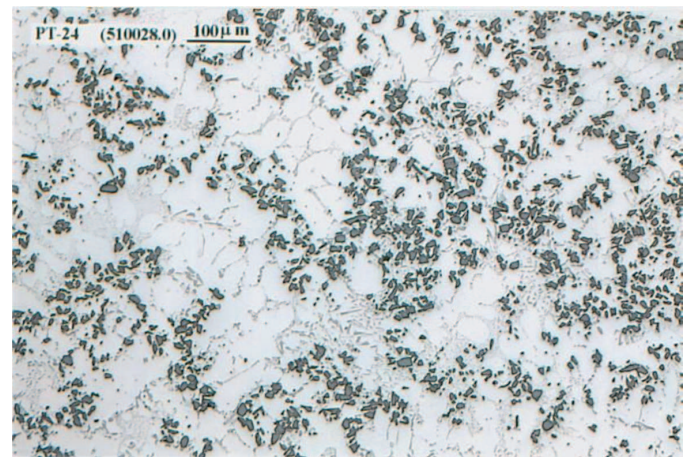


Fig. 7. Microstructure of the Al-Si10Mg/SiC_{20p}

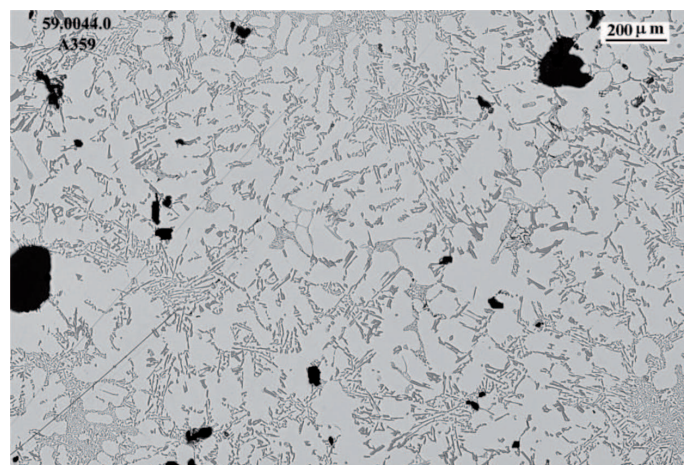


Fig. 8. Microstructure of the Al-Si9Mg alloy showing some large pores in it

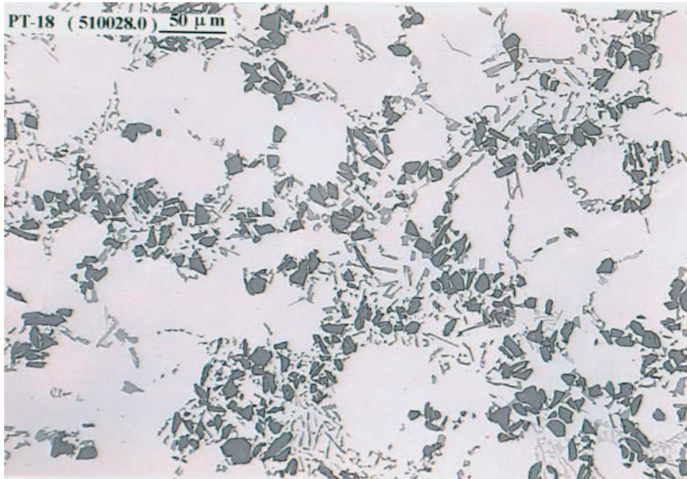


Fig. 9. Detail of the microstructure of the Al-Si10Mg/SiC_{20p}

Figure 9 shows a detail of the microstructure of the composite material. SiC particles are distributed along the sample even though they appear mainly located in the grain boundary region. This phenomenon is typical of particulate reinforced MMCs solidified in low solidification rate conditions. Instead of getting engulfed by the growing α -aluminium grains they get pushed by the solidification front [11-13, 18-21] within the sample and there is not any evidence of large pores in it. Al-Fe-Si intermetallic phases are more spherical, smaller and less frequent than in the unreinforced alloy.

Mechanical properties

Subsequently new samples were cast with the artificial cooling with water flow and natural cooling conditions to measure their mechanical properties and to compare them with the unreinforced alloy, see Table 3. Tensile tests were carried out in accordance to the UNE-EN 10.002.1 standard. The results show the average of 5 cylindrical specimens with a diameter of $8 \pm 0,12$ mm, $L_0 = 45$ mm, $R = 5$ and $L = 60$ mm.

TABLE 3

Mechanical properties of Al-Si10Mg/SiC_{20p} and the Al-Si9Mg alloys. The figure in parenthesis reflects the standard deviation

	UTS (MPa)	YS (MPa)	E (GPa)	Elong. (%)
Al-Si10Mg/SiC _{20p}	145 (12.2)	90 (4.2)	75 (0.6)	0.5-1 (0.2)
Al-Si10Mg/SiC _{20p} artificial cooling	150 (8.2)	110 (3.5)	80 (0.5)	1-1.8 (0.3)
Al-Si9Mg	130 (10.5)	80 (4.0)	70 (0.7)	3 (0.6)

A slight increase in the mechanical properties was measured in the reinforced material probably achieved through strengthening mechanisms associated with such

composite materials such as the increase in the density of dislocations produced by the mismatch of the CTE [22-27] of the matrix and the ceramic particles or the load transference to the particles. The homogeneity in the porosity distribution and decrease in the presence of large pores in the composite samples appreciated in the metallographic observations must also play an important role in the measured increase in mechanical properties. However the MMC presents low ductility values that may be related to the presence of particulates agglomerates and fracture of SiC particulates during the tensile tests.

4. Conclusions

Al-Si10Mg/SiC_{20p} material samples have been obtained through plaster casting under different processing conditions. The effect of the solidification rate on mechanical properties has been analysed. The comparison with the corresponding unreinforced Al-Si9Mg alloy has permitted to investigate the effect of the SiC particulates on the solidification pattern of the reinforced alloy as well as on the final microstructure and properties. The main conclusions from the work are following summarized:

Plaster casting process is suitable for the production of sound Al-Si composite materials having up to 20 vol.% of SiC particles that might be used for structural light components in aeronautical, automotive or electronic applications.

SiC particles have a strong influence on the solidification of the alloy. Solidification curves are shorter and all the main solidification events except the growth of aluminium dendrites start earlier and at higher temperatures. These results might be related to the decrease in the latent heat available during phase changes.

SiC particles play a role in the nucleation of the eutectic silicon and AlFeSi intermetallics and have a positive effect on the elimination of large pores.

Acknowledgements

Part of the results of this work were obtained in the frame of the research project IMINCAST (Contract number G1ST-CT-2002-50268) partially funded by the European Commission. The Danish company Temponik A/S collaborated in the design of the moulds and interpretation of the results.

REFERENCES

- [1] M.K. S u r a p p a, Aluminium matrix composites: Challenges and opportunities, Sadhana-Acad. P. Eng. **28**, 319 (2003).

- [2] B. Mondal, S. Kundu, A.K. Lohar, B.C. Pai, Net-shape manufacturing of intricate components of A356/SiC_p composite through rapid-prototyping-integrated investment casting, *Mater. Sci. Eng.* **498**, 37 (2008).
- [3] B. Ralph, H.C. Yuen, W.B. Lee, The processing of metal matrix composites – an overview, *J. Mater. Process Technol.* **63**, 339 (1997).
- [4] B. Previtali, D. Poggi, C. Taccardo, Application of traditional investment casting process to aluminium matrix composites, *Composites* **39**, 1606 (2008).
- [5] C. González-Rivera, J. Baez, R. Chávez, O. Alvarez, J. Juárez-Islas, Effect of SiC_p content on cooling curve characteristics and solidification kinetics of Al-Si/SiC_p cast composites, *Int. J. Cast Metal Res.* **16** (6), 531 (2003).
- [6] Y.M. Youssef, R.W. Hamilton, R.J. Dashwood, P.D. Lee, Latent heat evolution from TiB₂ particulate reinforced aluminium alloys, *Mater. Sci Forum.* **396**, 259 (2002).
- [7] C. Bartels, D. Raabe, G. Gottstein, U. Huber, Investigation of the precipitation kinetics in an Al6061/TiB₂ metal matrix composite, *Mater. Sci. Eng.* **A237**, 12 (1997).
- [8] J.K. Kim, P.K. Rohatgi, Nucleation on ceramic particles in cast metal matrix composites, *Metall. Mater. Trans A.* **31** **84**, 1295 (2000).
- [9] L.Y. Zhang, Y.H. Jiang, Z. Ma, S.F. Shan, Y.Z. Jia, C.Z. Fan, W.K. Wang, Effect of cooling rate on solidified microstructure and mechanical properties of aluminium-A356 alloy, *J. Mater. Process Tech.* **207**, 107 (2008).
- [10] A.M. Samuel, H. Liu, F.H. Samuel, Effect of melt, solidification and heat-treatment processing parameters on the properties of Al-Si-Mg/SiC_p composites, *J. Mater. Sci.* **28**, 6785 (1993).
- [11] A.M. Samuel, A. Gotmare, F.H. Samuel, Effect of solidification rate and metal feedability on porosity and SiC/Al₂O₃ particle distribution in an Al-Si-Mg (359) alloy, *Compos. Sci. Technol.* **53**, 301 (1995).
- [12] A. Dolata-Grosz, M. Dyzia, J. Sleziona, The formation of the structure of cast composites in different solidification conditions, *Arch. Mat. Sci. Eng.* **31**, 13 (2008).
- [13] J. Braszczyński, A. Zyska, Analysis of the influence of ceramic particles on the solidification process of metal matrix composites, *Mat. Sci. Eng.* **A278**, 195 (2000).
- [14] CTIF: Centre technique des industries de la fonderie, Atlas de micrographie quantitative des A-S7G, Editions techniques des industries de la fonderie (1976).
- [15] A.K. Kuruvilla, K.S. Prasad, V.V. Bhanuprasad, Y.R. Mahajan, Microstructure-property correlation in Al/TiB₂ composites, *Scripta Materialia* **24**, 873 (1990).
- [16] L. Bäckerud, G. Chai, J. Tamminen, Solidification characteristics of aluminium alloys, *Foundry alloys. AFS/Skanaluminium* **2**, ISBN 0-87433-119-6 (1990).
- [17] S. Nagarajan, B. Dutta, M.K. Surappa, The effect of SiC particles on the size and morphology of eutectic silicon in cast A356/SiC_p composites, *Compos. Sci. Technol.* **59**, 897 (1999).
- [18] Y.M. Youssef, R.J. Dashwood, P.D. Lee, Effect of clustering on particle pushing and solidification behaviour in TiB₂ reinforced aluminium PMMCs, *Composites: Part A* **36**, 747 (2005).
- [19] I.G. Watson, M.F. Forster, P.D. Lee, R.J. Dashwood, R.W. Hamilton, A. Chirazi, Investigation of the clustering behaviour of titanium diboride particles in aluminium, *Composites: Part A* **36**, 1177 (2005).
- [20] M.K. Surappa, Microstructure Evolution During Solidification of DRMMCs (Discontinuously Reinforced Metal Matrix Composites): State of Art, *J. Mater. Process Technol.* **63**, 325 (1997).
- [21] P. Bassani, B. Previtali, A. Tuissi, M. Vedani, G. Vimercati, S. Arnaboldi, Solidification and microstructure of A360-SiC_p cast composites, *Metallurgical Science and Technology* **23**, 1 (2003).
- [22] W.S. Miller, F.J. Humphreys, Strengthening mechanisms in metal matrix composites. Fundamental relationships between microstructure & mechanical properties of metal matrix composites, Edited by P.K. Law and M.N. Gunger, *The Minerals, metals and materials society* (1990).
- [23] F.J. Humphreys, A. Basu, M.R. Djazeb, The microstructure and strength of particulate metal-matrix composites, *Metal matrix composites-Processing, microstructure and properties*, 12th Riso International Symposium on materials science, 51 (1991).
- [24] N. Chawla, Y-L. Shen, Mechanical behaviour of particle reinforced metal matrix composites, *Adv. Eng. Mat.* **3**, 357 (2001).
- [25] T.W. Clyne, P.J. Withers, An introduction to metal matrix composites, Cambridge University Press, ISBN 0-521-41808-9 (1993).
- [26] M. Hu, W.-D. Fei, C.-K. Yao, A study on correlation of thermal mismatch stress of SiCw/Al composite through curves of thermal expansion coefficient, *Scripta Materialia* **46**, 563 (2002).
- [27] R.M. Aikín, Jr., The mechanical properties of In-situ composites, *JOM.* **49** (8), 35 (1997).